

Durham Research Online

Deposited in DRO:

28 November 2012

Version of attached file:

Published Version

Peer-review status of attached file:

Peer-reviewed

Citation for published item:

Wilkins, S. B. and Forrest, T. R. and Beale, T. A. W. and Bland, S. R. and Walker, H. C. and Mannix, D. and Yakhou, F and Prabhakaran, D. and Boothroyd, A. T. and Hill, J. P. and Hatton, P. D. and McMorrow, D. F. (2009) 'Nature of the magnetic order and origin of induced ferroelectricity in TbMnO₃.', Physical review letters., 103 (20). p. 207602.

Further information on publisher's website:

<http://dx.doi.org/10.1103/PhysRevLett.103.207602>

Publisher's copyright statement:

© 2009 American Physical Society

Additional information:

Use policy

The full-text may be used and/or reproduced, and given to third parties in any format or medium, without prior permission or charge, for personal research or study, educational, or not-for-profit purposes provided that:

- a full bibliographic reference is made to the original source
- a [link](#) is made to the metadata record in DRO
- the full-text is not changed in any way

The full-text must not be sold in any format or medium without the formal permission of the copyright holders.

Please consult the [full DRO policy](#) for further details.

Nature of the Magnetic Order and Origin of Induced Ferroelectricity in TbMnO_3

S. B. Wilkins,¹ T. R. Forrest,² T. A. W. Beale,³ S. R. Bland,³ H. C. Walker,^{2,4} D. Mannix,⁵ F. Yakhou,⁴ D. Prabhakaran,⁶
A. T. Boothroyd,⁶ J. P. Hill,¹ P. D. Hatton,³ and D. F. McMorrow²

¹Department of Condensed Matter Physics and Materials Science, Brookhaven National Lab, Upton, New York 11973-5000, USA

²London Centre for Nanotechnology, University College London, Gower Street, London WC1E 6BT, United Kingdom

³Department of Physics, Durham University, South Road, Durham, DH1 3LE, United Kingdom

⁴European Synchrotron Radiation Facility, Boîte Postal 220, F-38043 Grenoble CEDEX, France

⁵Institut Néel, CNRS-UJF, BP166, 38042 Grenoble, France

⁶Department of Physics, University of Oxford, Clarendon Laboratory, Parks Road, Oxford OX1 3PU, United Kingdom

(Received 9 June 2009; published 12 November 2009)

The magnetic structures which endow TbMnO_3 with its multiferroic properties have been reassessed on the basis of a comprehensive soft x-ray resonant scattering (XRS) study. The selectivity of XRS facilitated separation of the various contributions (Mn L_2 edge, Mn $3d$ moments; Tb M_4 edge, Tb $4f$ moments), while its variation with azimuth provided information on the moment direction of distinct Fourier components. When the data are combined with a detailed group theory analysis, a new picture emerges of the ferroelectric transition at 28 K. Instead of being driven by the transition from a collinear to a noncollinear magnetic structure, as has previously been supposed, it is shown to occur between two noncollinear structures.

DOI: 10.1103/PhysRevLett.103.207602

PACS numbers: 77.80.-e, 71.27.+a, 75.25.+z, 77.84.-s

Recently, considerable interest has been focused on a class of materials called multiferroics [1], that display strongly coupled magnetic and ferroelectric order parameters. Of particular significance is the fact that ferroelectricity results from phase transitions between different magnetic structures [2–5] which allows the ferroelectric state to be controlled by the application of an external magnetic field [3,6,7]. Developing a microscopic understanding of these effects represents a considerable challenge from a fundamental physics perspective, while their exploitation may lead to novel devices [1]. Various theoretical approaches [8,9] have shown that a detailed, microscopic knowledge of the magnetic structures is of central importance in understanding the multiferroics.

In TbMnO_3 , ferroelectricity occurs below 28 K, concomitant with a transition between two magnetic phases [10]. Using neutron diffraction, Kenzelmann *et al.* [4] proposed that at this temperature the Mn magnetic moments undergo a collinear to noncollinear transition, forming a cycloid which removes an inversion center resulting in a ferroelectric polarization.

Here we measure reflections in addition to the $(0, \tau, 1)$ type observed in Ref. [4], utilizing soft x-ray resonant scattering. This allows us to definitively measure the Fourier components with element specific sensitivity. We consider all observed reflections to be Fourier components of a single magnetic structure and find that the transition associated with ferroelectricity is not one from a collinear to noncollinear cycloidal magnetic structure, as has been previously reported [4], but that the transition actually corresponds to one between two noncollinear magnetic structures, where below 28 K there exists a cycloidal component.

In previous work, neutron diffraction measurements [4,11,12] have shown three magnetic transitions. Below $T_{N1} = 42.5$ K the Mn^{3+} ions develop long range order. In the work of Kajimoto *et al.* [11], magnetic superlattice reflections were observed at $(0, \tau, l)$ and $(0, 1 - \tau, l)$ type positions with l integer and $\tau = 0.27$. At $T_{N2} = 28$ K there is a second magnetic transition which coincides with the appearance of a spontaneous electric polarization along the c axis. Finally, the Tb ions order below a third transition at $T_{Tb} = 7$ K. Kenzelmann *et al.* [4], developed an appealing model of the magnetic structure whereby above T_{N2} the magnetic moments on the Mn ions are polarized along the b axis in an incommensurate, collinear fashion, and argued that at T_{N2} the magnetic moments on the Mn sites rotate to form an elliptical cycloid in the bc plane. This noncollinear structure causes a finite ferroelectric polarization along the c axis. Hard x-ray scattering experiments have been performed on TbMnO_3 [13–15], and report both nonresonant and resonant magnetic satellites at $(0, \tau, l)$, $(0, 1 - \tau, l)$ type locations. However, for these experiments the resonances used do not provide direct information on the localized Mn $3d$ or Tb $4f$ states which are of principal interest for understanding the magnetic order [16–18]. The soft x-ray resonant scattering experiments reported here overcome this limitation by probing these states directly [19–23].

Experiments were carried out on beam lines 5U1 at the SRS, Daresbury Laboratory, U.K. and ID08, European Synchrotron Radiation Facility, France. Two crystals with the $(0, 1, 0)$ and $(0, 0.28, 1)$ surface normal were used, cut from the same boule as used previously [13,24]. Unless otherwise noted, the incident photon energy was tuned to the L_2 edge of Mn, to select the magnetic scattering from

the manganese. The polarization of the incident x rays was chosen to be perpendicular to the scattering plane (σ polarization).

Figure 1 shows a scan taken at 20 K along the $(0, 1, 0)$ direction in reciprocal space from the crystal with $(0, 1, 0)$ surface normal. Three superlattice reflections are visible at $(0, \tau, 0)$, $(0, 2\tau, 0)$, and $(0, 1 - 2\tau, 0)$ with $\tau \approx 0.28$. All three reflections were found to resonate at the L_2 and L_3 edges of Mn and were not visible off resonance. We assign the $(0, \tau, 0)$ reflection to incommensurate ordering of the magnetic moments on the Mn sites and the $(0, 2\tau, 0)$ to be the second harmonic from the resonant x-ray cross section [25,26]. The $(0, 1 - 2\tau, 0)$ reflection corresponds to the second harmonic from the $(0, 1 - \tau, 0)$ reflection. Upon cooling the sample with the $(0, 0.28, 1)$ reflection surface normal, and tuning the photon energy to the Tb M_4 edge, a superlattice reflection was observed at $(0, \tau, 1)$ with $\tau \approx 0.28$ below 28 K. This reflection is not accessible at the Mn L edges, but was visible at the Tb M_5 and M_4 edges with no intensity observed off resonance.

The temperature dependence of the integrated intensity of the $(0, \tau, 0)$, $(0, 2\tau, 0)$, and $(0, 1 - 2\tau, 0)$ reflections at the Mn L_2 edge is shown in Fig. 2(a). Here a clear transition is seen at T_{N1} , below which the intensity of the $(0, \tau, 0)$ grows. At T_{N2} , a further transition is observed at which the intensity of the $(0, \tau, 0)$ reflection is found to increase more rapidly. Turning to the $(0, 2\tau, 0)$ and $(0, 1 - 2\tau, 0)$ reflections, these are only observed below a temperature of ≈ 35 K. On cooling below 35 K their intensities increase, first gradually then more rapidly below T_{N2} . Upon cooling below T_{N1} , τ decreases in an almost linear fashion, as shown in Fig. 2(b), until T_{N2} where the value stabilizes at approximately $\tau = 0.287$, although it does not lock in. Identical behavior was seen in τ from all reflections. Finally, Fig. 2(a) also shows the integrated intensity of the $(0, \tau, 1)$ reflection measured at the Tb M_4 edge. This reflection is only visible below T_{N2} . The presence of the Tb resonant signal is an explicit confirmation of a finite Tb moment in the low T phase, as inferred previously [4,27].

It is possible to determine the magnetic moment direction by utilizing the fact that the scattered intensity is a

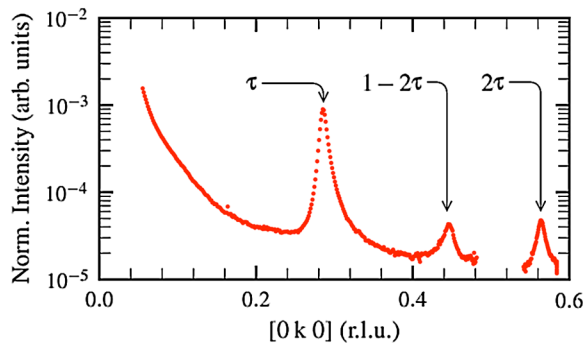


FIG. 1 (color online). Scan along the $[010]$ direction in reciprocal space at an incident photon energy corresponding to the L_2 edge of Mn. r.l.u. denotes reciprocal-lattice units.

function of the projection of the moment along the scattered x-ray direction and the scattering geometry [25]. In a diffraction experiment, one measures the direction of the *Fourier component* of the magnetic structure as determined by the \mathbf{Q} vector chosen. To determine the direction of all Fourier components present, we measured the azimuthal dependence (the rotation of the sample around the \mathbf{Q} vector) of all observed Mn wave vectors. No measurement of the scattered polarization was made.

Figure 3 shows the azimuthal dependence of the $(0, \tau, 0)$, $(0, 2\tau, 0)$, and $(0, 1 - 2\tau, 0)$ reflections as measured at the Mn L_2 edge. In the top panel, the $(0, \tau, 0)$ reflection is shown at 26 K (red circles) and 32 K (blue squares). While the maximum integrated intensity changes between these two temperatures, the functional form is identical, indicating that the direction of this Fourier component does not change across T_{N2} . This azimuthal dependence can be fitted to the form $I_\tau(\psi) = A \cos^2 \psi$, where A is a proportionality constant and ψ is the azimuthal angle. $\psi = 0$ corresponds to the condition where the $[001]$ direction lies in the scattering plane. We can immediately exclude a b -axis direction for this Fourier component, since this is parallel to the \mathbf{Q} and thus would be invariant under rotations around \mathbf{Q} . The zero in intensity at $\psi = 90^\circ$ (corresponding to the case where the c axis is perpendicular to the scattering plane) implies that the magnetic moment has no projection along the outgoing x ray at this azimuth, and

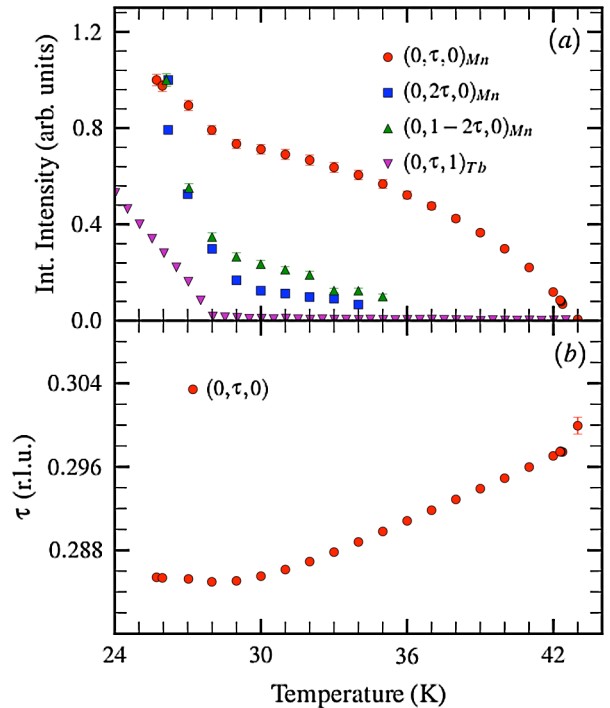


FIG. 2 (color online). (a) Temperature dependence of the integrated intensity of the $(0, \tau, 0)$, $(0, 2\tau, 0)$, and $(0, 1 - 2\tau, 0)$ measured at the Mn L_2 edge and the $(0, \tau, 1)$ measured at the Tb M_4 edge. (b) Temperature dependence of the incommensurability τ measured from the peak position of the $(0, \tau, 0)$ measured at the Mn L_2 edge.

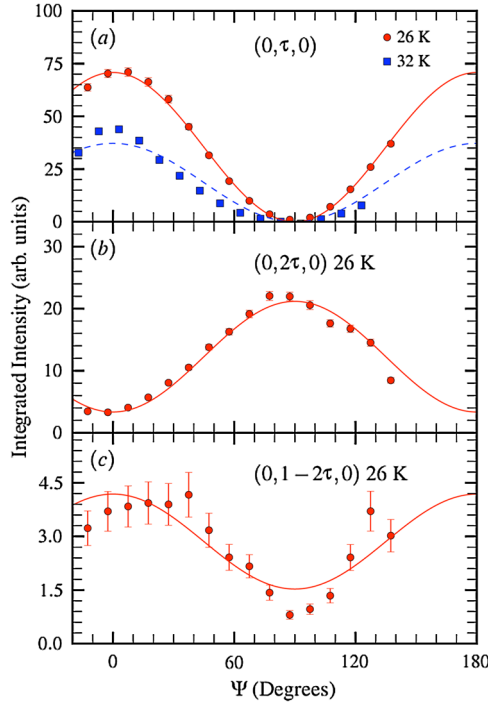


FIG. 3 (color online). Azimuthal dependence of the (a) $(0, \tau, 0)$, (b) $(0, 2\tau, 0)$, and (c) $(0, 1 - 2\tau, 0)$ superlattice reflections at the Mn L_2 edge in the noncollinear phase at 26 K (red circles). The azimuthal dependence of the $(0, \tau, 0)$ at 32 K in the collinear phase is shown for comparison in the top panel (blue squares). The red solid (blue dashed) lines show simulations to the azimuthal dependencies at 26 K (32 K). The origin of the azimuth corresponds to the condition where the $[001]$ direction lies in the scattering plane.

this means the a - and b -axis components are strictly zero at this wave vector. Thus this Fourier component is along the c axis. This result is confirmed by the azimuthal dependence of the $(0, 2\tau, 0)$ signal at 26 K shown in Fig. 3. This can be fitted to the form $I_{2\tau}(\psi) = A' + B'[\sin^4\psi + \sin^2\psi\cos^2\psi]$. With the assumption that this reflection is the second harmonic from the resonant x-ray cross section [25], this is also consistent with a Fourier component along the c axis. The finite offset, introduced through the A' coefficient is due to scattering from the lattice distortion induced by the magnetic order. This is a pure charge resonant signal and has no azimuthal dependence. No scattering was observed off resonance.

The $(0, 1 - 2\tau, 0)$ azimuthal scan can be fitted to the form $I_{1-2\tau}(\psi) = A'' + B''[\cos^4\psi + \cos^2\psi\sin^2\psi]$. This form is similar to that of the $(0, 2\tau, 0)$ signal but with a $\frac{\pi}{2}$ phase shift. Thus the Fourier component at $(0, 1 - 2\tau, 0)$ and therefore at $(0, 1 - \tau, 0)$, is along the a axis. Voigt *et al.* [15], observed both reflections of the $(0, \tau, 0)$ and $(0, 1 - \tau, 0)$ type at the Tb L edges where a similar $\frac{\pi}{2}$ phase shift was observed. However, this only confirms the presence of a polarization of the Tb $5d$ states at this wave vector. Our data prove that these wave vectors correspond to ordering of the Mn ions.

In summary, we conclude that at 26 K, the magnetic structure possesses Fourier components at $(0, \tau, 0)$ and $(0, 1 - \tau, 0)$ which are along the principal c and a axes, respectively, in addition to the b -axis and c -axis components reported previously at $(0, \tau, 1)$ [4].

To explain the presence of these Fourier components, and the previous neutron results [4] one might turn to a model of magnetic domains in which different parts of the sample have different ordering wave vectors. Instead, we propose that these reflections arise from one coherent magnetic structure which explains all the observed wave vectors. This is because (i) the incommensurability is the same and has the same temperature dependence at all reflections, and is consistent with that measured by neutrons [4,11] and nonresonant x rays [13,15]. This would seem unlikely if the reflections originated from different parts of the sample with different physical characteristics. (ii) The $(0, \tau, 0)$ wave vector shows magnetic transitions at 41 K and at 28 K; that is, it exhibits transitions entirely consistent with those observed at the $(0, \tau, 1)$ wave vector [4] again suggesting they have a common origin. (iii) Such a coherent structure is consistent with the symmetry analysis performed by Kenzelmann *et al.* [4]. Finally, we note our sample does indeed show the cycloidal ordering below 28 K, which we observe at the $(0, \tau, 1)$ wave vector. We can thus rule out the possibility that this sample somehow differs from others and is not multiferroic.

We now construct these new magnetic structures. For the high-temperature phase above 28 K, we start from the model of Kenzelmann *et al.* [4], who found a single Γ_3 component along the b axis with a wave vector of $(0, \tau, 1)$. We add to this the $(0, \tau, 0)$ c -axis Fourier component observed here. This introduces a canting of the spins away from the b axis. Further, this canting must be ferro ordered along the c axis, since this Fourier component is observed at even integer l values. We estimate the canting angle from the neutron intensities of Kajimoto *et al.* [11], to be approximately 5° away from the b axis. This new structure is noncollinear and is shown with this canting angle in Fig. 4(a). Note, this structure is consistent with the group theory presented by Kenzelmann *et al.* [4]. If we examine the Γ_3 irreducible representation of the little group G_k of the wave vector $(0, k, 0)$ from the crystallographic space group $Pbnm$, we find that the symmetry operation m_{xy} at $z = \frac{1}{4}$ relates two Mn spins along the c axis and has a character of 1. For a b -axis Mn magnetic moment, this symmetry operator flips the spin, resulting in an antiferro arrangement along the c axis (odd integer l). On the other hand, for a c -axis component, this same operator leaves the spin invariant (ferro along c and peaks at even integer l). Therefore in a canted structure with Fourier components present at odd and even integer l values, these must see the b -axis and c -axis moment directions, respectively—as is observed.

Turning now to the low temperature structure, we again start from the model of Kenzelmann *et al.* [4], who found a

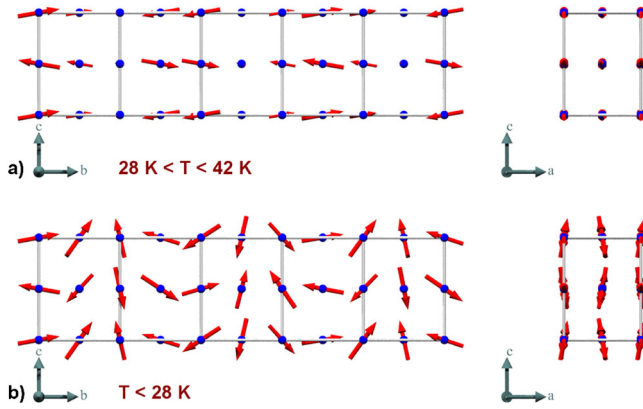


FIG. 4 (color online). (a) Proposed magnetic structure in the region $28\text{ K} < T < 41\text{ K}$ projected onto both the crystallographic b - c (left) and a - c (right) planes. (b) Proposed magnetic structure below 28 K .

single Fourier component of $(0, \tau, 1)$ with both Γ_2 and Γ_3 components with moment directions along the c axis and b axis, respectively. We add to this the $(0, \tau, 0)$ c -axis component, as in the high temperature phase, and the $(0, 1 - \tau, 0)$ a -axis Fourier component. The fact that this latter reflection is a satellite of the $(0, 1, 0)$ *forbidden* Bragg reflection, implies that this component is arranged antiferromagnetically along the b axis. Thus this $(0, 1 - \tau, 0)$ a -axis component causes a canting of the Mn moments towards the a axis that is antiferro ordered along the $[010]$ direction. From the ratio of the azimuthal maxima of the $(0, 2\tau, 0)$ and $(0, 1 - 2\tau, 0)$ peaks we estimate the ratio of the a -axis component to the c -axis component to be ~ 0.66 . These a -axis and c -axis Fourier components then modify the cycloid of Kenzelmann *et al.* and the resulting structure is shown in Fig. 4(b).

The addition of the $(0, 1 - \tau, 0)$ component is consistent with a Γ_2 representation. The Mn spins along the b axis are related by the b glide (m_{yz}) and the twofold screw axis 2_y . In the Γ_2 representation, the characters of these operators are -1 and 1 , respectively. For an a -axis spin, then, Γ_2 will have an antiparallel alignment to b -axis neighbors and therefore a wave vector of the $(0, 1 - \tau, 0)$ type. For the $(0, \tau, 0)$ c -axis component, the same analysis as was discussed above in the high-temperature phase also applies below 28 K and it is a Γ_3 component. Thus this new low temperature structure is also consistent with Kenzelmann *et al.* with both Γ_2 and Γ_3 components. We note that the $(0, 1 - 2\tau, 0)$ reflection is also present in the high-temperature phase. While the intensity is too weak to carry out azimuthal analysis, symmetry arguments suggest that it remains an a -axis component, in which case it would be a Γ_2 component and both representations would be present above 28 K too.

In conclusion, we propose new magnetic structures above and below 28 K in TbMnO_3 . Specifically, our data require the addition of a -axis and c -axis components, with Fourier components $(0, 1 - \tau, 0)$ and $(0, \tau, 0)$, respectively.

These new components are present in both the high-temperature and low-temperature phases and mean that the ferroelectrically relevant transition at 28 K is not, as previously reported, from a collinear structure to noncollinear one, but rather both phases are noncollinear and both are described by Γ_2 and Γ_3 irreducible representations. The essential difference then in the ferroelectric phase is the cycloidal component to the magnetic structure that forms in the Γ_2 component. We emphasize that the new components do not change the direction of the ferroelectric polarization. Our magnetic structure reconciles all observed wave vectors into a single coherent structure, and therefore disagrees with a model of coexistence, as suggested by Kajimoto *et al.* [11], and a model of domains as suggested by Mannix *et al.* [13].

The authors would like to thank S.J. Billinge, E.S. Božin, B. Detlefs, C. Detlefs, W. Ku, and A. Wills for many stimulating discussions. The work at Brookhaven National Laboratory is supported by the Office of Science, U.S. Department of Energy, under Contract No. DE-AC02-98CH10886. Work at UCL was supported by the EPSRC and the Royal Society and in Durham and Oxford by the EPSRC.

-
- [1] D. Khomskii, *Physics* **2**, 20 (2009).
 - [2] T. Kimura *et al.*, *Nature (London)* **426**, 55 (2003).
 - [3] N. Hur *et al.*, *Nature (London)* **429**, 392 (2004).
 - [4] M. Kenzelmann *et al.*, *Phys. Rev. Lett.* **95**, 087206 (2005).
 - [5] G. Lawes *et al.*, *Phys. Rev. Lett.* **95**, 087205 (2005).
 - [6] N. Aliouane *et al.*, *Phys. Rev. B* **73**, 020102(R) (2006).
 - [7] J. Strempler *et al.*, *Phys. Rev. B* **78**, 024429 (2008).
 - [8] H. Katsura, N. Nagaosa, and A. V. Balatsky, *Phys. Rev. Lett.* **95**, 057205 (2005).
 - [9] M. Mostovoy, *Phys. Rev. Lett.* **96**, 067601 (2006).
 - [10] T. Kimura *et al.*, *Phys. Rev. B* **71**, 224425 (2005).
 - [11] R. Kajimoto *et al.*, *Phys. Rev. B* **70**, 012401 (2004).
 - [12] S. Quezel *et al.*, *Physica (Amsterdam)* **86B-88B**, 916 (1977).
 - [13] D. Mannix *et al.*, *Phys. Rev. B* **76**, 184420 (2007).
 - [14] O. Prokhnenko *et al.*, *Phys. Rev. Lett.* **99**, 177206 (2007).
 - [15] J. Voigt *et al.*, *Phys. Rev. B* **76**, 104431 (2007).
 - [16] M. Usuda, J. I. Igarashi, and A. Kodama, *Phys. Rev. B* **69**, 224402 (2004).
 - [17] K. Kuzushita *et al.*, *Phys. Rev. B* **73**, 104431 (2006).
 - [18] D. Mannix *et al.*, *Phys. Rev. Lett.* **86**, 4128 (2001).
 - [19] S. B. Wilkins *et al.*, *Phys. Rev. Lett.* **90**, 187201 (2003).
 - [20] T. A. W. Beale *et al.*, *Phys. Rev. B* **75**, 174432 (2007).
 - [21] S. B. Wilkins *et al.*, *Phys. Rev. Lett.* **91**, 167205 (2003).
 - [22] K. Thomas *et al.*, *Phys. Rev. Lett.* **92**, 237204 (2004).
 - [23] S. Dhesi *et al.*, *Phys. Rev. Lett.* **92**, 056403 (2004).
 - [24] T. R. Forrest *et al.*, *J. Phys. Condens. Matter* **20**, 422205 (2008).
 - [25] J. P. Hill and D. F. McMorrow, *Acta Crystallogr. Sect. A* **52**, 236 (1996).
 - [26] J. Hannon *et al.*, *Phys. Rev. Lett.* **61**, 1245 (1988).
 - [27] F. Fabrizi *et al.*, *Phys. Rev. Lett.* **102**, 237205 (2009).